Research Article

Yan Yin, Hong Mai, Li-Ying Zhang, Yan Liao, Xu-Peng Liu, Ye-Ping Wei*

A Zn(II)–organic cage with semirigid ligand for solvent-free cyanosilylation and inhibitory effect on ovarian cancer cell migration and invasion ability via regulating mi-RNA16 expression

https://doi.org/10.1515/chem-2020-0144
received March 04, 2020; accepted June 09, 2020

Abstract: $[Zn_6(L)_4(DMF)_2(H_2O)_4](1,4\text{-Dioxane})_2(DMF)_{10}(H_2O)_4$ (**1**, L = 4,4′,4″-(benzene-1,3,5-triyltris(oxy))tribenzoate), the metal-organic cage, was produced via $Zn(NO_3)_2{\cdot}6H_2O$ reacting with the H_3L ligand in the mixed solvent of DMF and water. The heterogeneous catalytic activities of the complex **1** for the aldehydes cyanidation under the conditions of free solvent were studied, which indicates that the removal of coordination solvents could greatly improve the catalytic activities. Furthermore, the inhibitory effect of the compound against the ovarian cancer cells was assessed. The mi-RNA16 relative expression level was measured after exposure to the compound with real-time reverse transcription-polymerase chain reaction. The invasion and migration of cells after compound treatment were also detected by the transwell method.

Keywords: metal-organic cage, paddle-wheel cluster, cyanosilylation reaction, ovarian cancer

1 Introduction

Micro RNA (micro RNA, mi RNA) is a group of endogenous noncoding small molecular RNAs of about 21–23 nucleotides in length that are widely found in eukaryotes [1]. They are involved in the regulation of gene post-transcriptional levels and have a very significant function in the apoptosis and differentiation of cells. More and more studies have shown that changes in mi RNA expression levels are related to the pathogenesis and progression of a variety of human malignancies, for instance, ovarian cancer, cervical cancer, as well as colorectal cancer [2,3]. The miRNA abnormal expression in ovarian cancer is closely related to its occurrence, development, metastasis, drug resistance, and prognosis [4]. It is expected to become a marker for early diagnosis and prognosis of ovarian cancer and provide a new clinical analysis for chemotherapy resistance and personalized treatment ideas.

The cyanation of carbonyl compounds involving the trimethylsilyl cyanide (TMSCN) is a direct and effective method to generate the C–C bond in the organic synthesis. In recent years, cyanohydrin has been widely concerned because it is the key intermediate for synthesizing the biologically significant compounds (for instance, the α-hydroxy acids, α-hydroxyl ketones as well as α-amino acids) [5–7]. Most researches have revealed that this reaction is catalyzed through homogeneous catalysts (i.e., metal Lewis acids/bases, inorganic solid acids/bases, and the nonmetallic organic molecules), but their performances are still limited and difficult to be separated and recovered [8–10]. Metal-organic polyhedron (MOP) is a kind of discrete container molecules and assembled via functional organic ligands and metal ions by the coordination bonds. As the basic sequence of nanochannels, nanocontainers, and porous materials, MOPs have been extensively studied [11–14]. In recent years, MOPs have been extensively utilized for many organic reactions as catalytic centers. For example, Li and his colleagues have reported the ring-opening of styrene oxide promoted via the MOP [15]; Wang and co-workers have applied an In(III)–MOP as the heterogeneous catalyst in Strecker reaction of aminonitriles and CO_2 cycloaddition [16]. In this research, $[Zn_6(L)_4(DMF)_2(H_2O)_4](1,4\text{-dioxane})_2(DMF)_{10}(H_2O)_4$ (**1**, L = 4,4′,4″-(benzene-1,3,5-triyltris(oxy))tribenzoate), the metal-organic cage, was triumphantly produced through the reaction between H_3L ligand and $Zn(NO_3)_2{\cdot}6H_2O$ in the mixed solvent of DMF and water. The complex **1**'s heterogeneous catalytic activities for the

* **Corresponding author: Ye-Ping Wei,** Department of Gynaecology, Second Affiliated Hospital of Guangxi Medical University, Nanning 530021, China, e-mail: wyeping_12@126.com
Yan Yin, Hong Mai, Li-Ying Zhang, Yan Liao, Xu-Peng Liu: Department of Gynaecology, Second Affiliated Hospital of Guangxi Medical University, Nanning 530021, China

cyanosilylation of aldehydes under the solvent-free conditions were studied, which reveals that the removal of coordination solvents could greatly improve the catalytic activities. In the biostudy, the anticancer activity of the compound against the cancer cells was evaluated via the transwell assay and reverse transcription-polymerase chain reaction. The real-time RT-PCR results indicated that the compound could significantly increase the expression level of mi-RNA16 in a time-dependent manner, which is important to inhibit the cancer cell progression. In addition to this, the results for the invasion and migration of cancer cells also suggested that the compound reveals an outstanding inhibitory effect against cancer cells.

2 Experimental

2.1 Chemicals and measurements

The reagents and solvents utilized in this research were acquired from the market, and then they were utilized without additional purification unless otherwise specified. We commonly can utilize the spectrometer of Bruker tensor 27 to record the fourier transform infrared spectroscopy spectra from 4,000 to 400 cm^{-1} utilizing the KBr pellets, which averaged 8 scans. Utilizing the Elemental analyzer of Elementar Vario-EL CHN to analyze the elements of Nitrogen, Hydrogen, as well as Carbon for complex in the fresh samples. A 3H-2000PS analyzer (Beishide, China) was utilized for the measurement of gas adsorption. The measurement of sorption was kept by the liquid nitrogen at 77 K. The yield for the separated product was detected via the GC-MS equipment (Agilent 5977B).

2.2 Preparation and characterization for $[Zn_6(L)_4(DMF)_2(H_2O)_4](1,4\text{-}Dioxane)_2(DMF)_{10}(H_2O)_4$ (1)

We mixed 0.029 g and 0.1 mmol $Zn(NO_3)_2{\cdot}6H_2O$, H_3L (0.05, 0.0243 g), DMF (1.5 mL), as well as 1,4-dioxane (1.5 mL) solution to form a mixture and stirred it for 10 min. After that, two drops of 1 mol/L HNO_3 was added. Then, the solution was transferred to a 23 mL glass reactor and heated to 85°C. After 15 h, cooling the system to the ambient temperature and colorless bulk crystals were obtained. Elemental analysis (%) for **1** ($C_{152}H_{176}N_{12}O_{60}Zn_6$): N, 4.77%; H, 5.04%; C, 51.82%. Found: N, 4.69%; H, 4.96%; and C, 51.48%.

We utilized the diffractometer of Oxford XcaliburE to get the data of X-ray. And we can analyze the data of strength through utilizing the software of crysalispro, after that transformed the intensity data into the files of HKL. The complex's original skeleton models were built through utilizing SHELXS based on the direct manner [17] and then modified the model through the SHELXL-2014 in accordance with the least square manner [18]. Via utilizing the anisotropic parameters, all the atoms of nonhydrogen were refined. Afterward, the entire hydrogen atoms are geometrically fixed to C atom and they are connected to through utilizing the command of auto fixation. After the structural refinement, we found that the $R1$ value is still relatively large (0.107). The relatively large $R1$ value is attributed to the high thermal vibration of the ligands in the framework, which results in some relatively large U_{eq} values of the ligand atoms. Refining them using the disordered model is impossible because there are too many atoms in the asymmetry unit (more than 300). In addition, the highly disordered lattice solvents as well as the large void space also lead to the high residue Q peaks in the void spaces which could not be properly defined. The refinement along with the crystallographic parameters for the complex **1** is described in detail in Table 1.

2.3 Real-time RT-PCR

At the aim of detecting the mi-RNA16 relative expression level in ovarian cancer cells CP70, real-time RT-PCR was conducted in this current research. This preformation was under instructions' guidance as the former described. In short, the CP70 ovarian cancer cells were cultured in the incubator at 5% CO_2 and 37°C condition. When the cells have the confluence of 70%, we added compound into the cells for 12 h and then treated for 24 h. Next, discarded cell culture medium and cleaned cells by using PBS. We extracted total RNA in cells by the Trizol reagent according to protocols. In accordance with the experimental scheme, the total RNA was extracted via Trizol reagent. The concentration of total RNA was measured by the OD_{260}/OD_{280} ratio method, and then it was reverse transcribed into cDNA through the high capacity cDNA reverse transcription kit. Conclusively, the mi-RNA16 relative expression was detected via the synergy brands Green Master Mix after treated with the compound. The relative quantification was performed via

Table 1: The parameters of crystallography and the refinement for complex **1**

Empirical formula	$C_{228}H_{164}N_4O_{84}Zn_{12}$
Formula weight	5088.06
Temperature/K	293(2)
Crystal system	Triclinic
Space group	$P\bar{1}$
a/Å	22.6523(2)
b/Å	22.98210(15)
c/Å	24.0122(2)
α/°	118.2561(12)
β/°	89.9530(11)
γ/°	118.3320(12)
Volume/Å^3	9279.35(19)
Z	1
$\rho_{calc}g$/cm^3	0.911
μ/mm^{-1}	0.817
Reflections collected	1,43,040
Independent reflections	36,828 [R_{int} = 0.0598, R_{sigma} = 0.0688]
Data/restraints/parameters	36,828/0/1,485
Goodness-of-fit on F^2	1.263
Final R indexes [$I \geq 2\sigma(I)$]	R_1 = 0.1071, ωR_2 = 0.3142
Final R indexes [all data]	R_1 = 0.1209, ωR_2 = 0.3324
Largest diff. peak/hole/e Å^{-3}	1.21/−0.64
CCDC	1987145

utilizing the $2^{-\Delta\Delta Ct}$ approach for three times. All the obtained results were expressed as mean ± standard deviation.

2.4 Transwell assay

The inhibition of the compound against the migration and invasion of CP70 ovarian cancer cells was determined via the transwell approach based on the instruments with a little modification. Briefly, CP70 ovarian cancer cells in the logical growth stage were collected and inoculated into the upper chambers and cultured in free-FBS medium combined with the 10% FBS. We added complement couture medium into the lower chambers for incubation. Before the experiment, the transwell chambers of 24-well (Corning, NY, USA) were precoated without or with the matrigel matrix (BD Biosciences, NJ, USA) for the invasion and migration of cells, respectively. The plates were placed in the incubator at 5% CO_2 and 37°C condition for 1 day, on the upper membrane, the remained cells were removed, and the cells on the other side of the camber were labeled with the crystal violet (0.5%). Cells on the surface below the membrane were numbered and analyzed. All the results were presented as mean ± SD.

Ethical approval: The conducted research is not related to either human or animal use.

3 Results and discussion

3.1 Molecular structures

The complex **1**'s colorless bulk crystals can be acquired via the solvothermal reaction between H_3L and Zn $(NO_3)_2{\cdot}6H_2O$ in 1,4-dioxane and DMF mixed solvents at 85°C for 24 h, and its chemical formula was $[Zn_6(L)_4(DMF)_2(H_2O)_4](1,4\text{-dioxane})_2(DMF)_{10}(H_2O)_4$ according to the analysis of element and the single crystal diffraction of X-ray results. Complex **1** was insoluble in some common organic solvents such as the DMF, EtOH, and MeOH, which indicates that it might be applied as the heterogeneous catalyst for the organic reactions. In accordance with the data of crystal harvested at ambient temperature, the refinement and structural solution results indicated that the complex **1** is composed of discrete molecule cages, and it was crystallized in the space group $P\bar{1}$. The chemical formula of **1** is composed of two asymmetry units with a Z = 1. The asymmetry unit of **1** contains six Zn(II) ion, four ligand L^{3-}, two coordinated molecules of DMF, and four coordinated water molecules. According to Figure 1a, in the cage, Zn (II) ion is five-coordinated, which was completed by four oxygen atoms from four ligands along with an oxygen atom in the molecules of DMF or H_2O, forming a trigonal bipyramid configuration. The bond spacing of Zn(II)–O varies from 1.923(17) to 2.143(6) Å, which are analogous to the distance observed in other Zn(II)-based metal–organic complexes constructed from the carboxylate ligands [19–21]. Two neighboring Zn(II) ions are linked through four carboxylic acid groups and form a four-linked paddle-wheel node. Three zinc paddle wheel clusters coordinated by a ligand L^{3-} generate a three-linked node. It should be noted that owing to the ether bonds flexibility in the ligands of L^{3-}, these three coordination arms face the same side, generating a L^{3-} with claw-shape (Figure 1b). Six paddle-wheel nodes combined with eight L^{3-} ligands to generate the metal organic cage, the inner diameter of cage is 16 Å, and the window dimension of the cage is 9 Å (Figure 1c). For clarity, the four-linked $[Zn_2(COO)_4]^-$ impeddle wheel

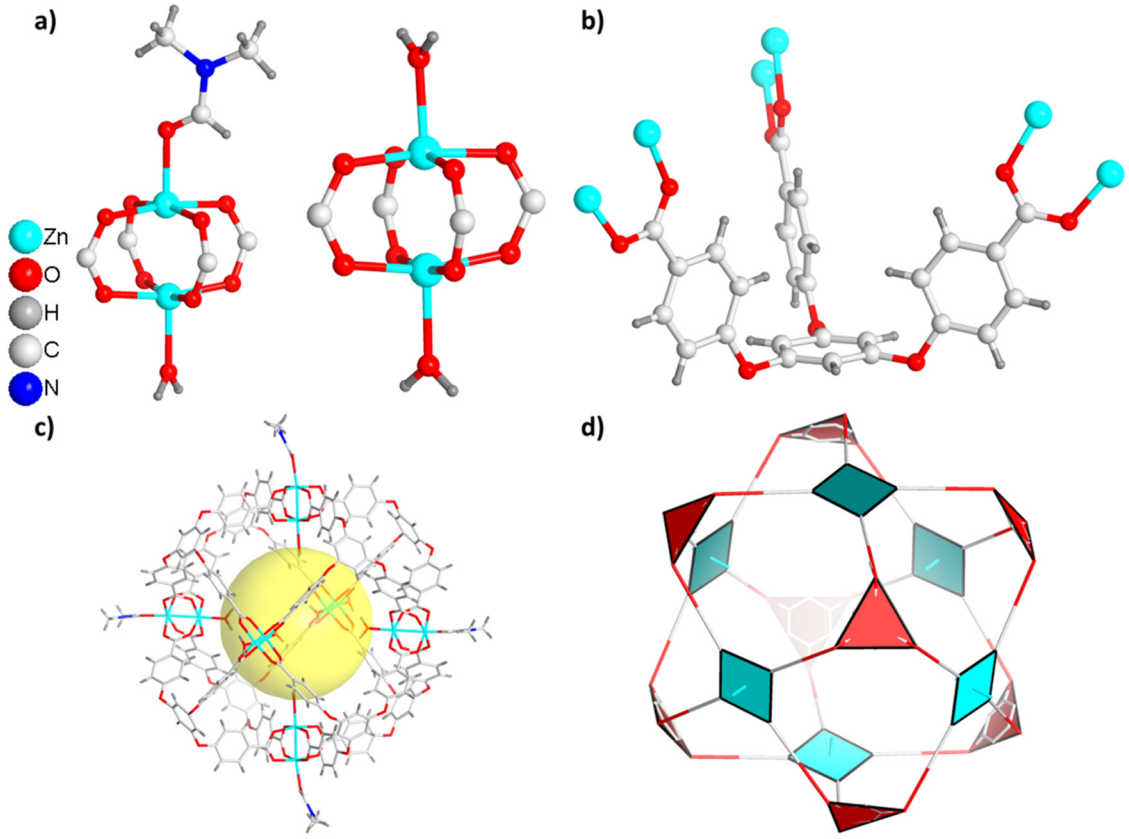

Figure 1: (a) View of the two different types of binuclear Zn clusters of **1** (the atom legend is shown in the left of this figure). (b) View for the coordinated mode view for ligand L^{3-}. (c) The cage type skeleton for the complex **1**. (d) The simplified network for complex **1**.

element can be simplified as the node of quadrangular, and the three-linked L^{3-} with claw-shape can be considered as a three-linked node, making the polyhedral cage (Figure 1d). The calculations of PLATON reveal that the volume of void is 4863.6 $Å^3$ (52.1% of 9335.1 $Å^3$ unit cell volume).

3.2 Catalytic studies

To test the products' phase purity, the experiments for the PXRD were conducted for these two complexes (Figure 2a). The peak positions of PXRD diagrams of the simulation and experiment are in line with each other, and this reflects that for the products of crystal with bulk-shape, crystal architectures are a real representative. The differences in the strength can attribute to the preference effects of the crystals. Meanwhile, to study the complex **1**'s thermal stability, the experiment of thermogravimetric analysis (TGA) was conducted between 25°C and 800°C at 10°C min^{-1} heating rate under nitrogen flow (Figure 2b). At 25°C to 220°C temperature range, the complex **1**'s curve of TGA reveals 34.2% continuous weightlessness, which may be owing to the removal of lattice solvents and coordination (with the calculated value of 33.9%). After 280°C, there is a second weight loss, which suggests that the organic ligands decomposition is accompanied by the collapse of the entire skeleton. As discussed earlier, the as-prepared complex **1** has a cage-type structure with large square windows and inner spaces. To establish the porosity of **1**, about 100 mg of the as-prepared samples was treated via the supercritical CO_2 for 12 h and then outgassed under a dynamic vacuum for another 12 h to provide activated **1** (hereinafter referred to as **1a**). The measurement of N_2 gas sorption at 77 K (Figure 2c) revealed the reversible isotherm with I-type, which is characterized by the microporous materials, and the microporous materials have high N_2 adsorption rate of 65 $cm^3 g^{-1}$. The surface area of BET was estimated at 155 $m^2 g^{-1}$. Meanwhile, the calculation of pore size distribution by HP approach reveals a pore size location around 0.86 nm, which matches well with that observed from the data of crystal (Figure 2d).

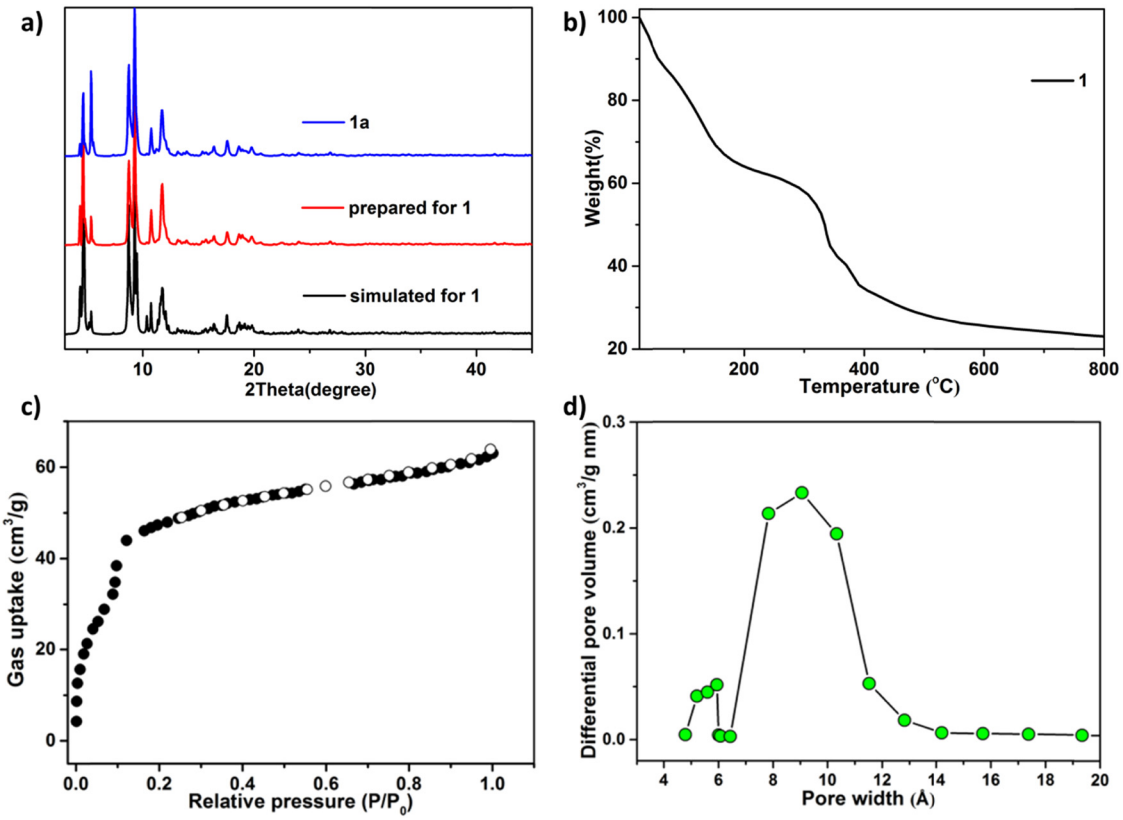

Figure 2: (a) The complex **1'**s patterns of PXRD; (b) the curve of TGA for the complex **1**; (c) the N_2 adsorption curve for the **1a** at 77 K; (d) the distribution of pore size for the **1a**.

In consideration that the complex **1a** possesses coordination unsaturated metal centers of unsaturated metal centres and large pores, it can be utilized as the potential Lewis acid catalyst for cyanidation of carbonyl compounds and its catalytic performance has been detected. In the condition of solvent-free, taking benzaldehyde as the standard molecule, the model experiment was conducted by changing the amount and temperature of the catalyst. It can be seen from Table 2 that complex **1a** revealed superb catalytic activity. The conversion of benzaldehyde was 98% in half a day at the ambient temperature (Figures S1 and S2), and the catalyst loading amount was 0.1 mol% zinc, which was only 1/15 of Cr-MIL-101 (the active position of Cr is 1.5 mol%) has the highest catalytic effect in the cyanogenation [22]. Besides, as the catalyst, complex **1a** does not need the dichloromethane organic solvent, whereas catalyst Cr-MIL-101 does. After 120 min, the reaction was stopped absolutely via filtration and removal of the complex **1a**, and only 45% of total conversion was provided after 15 h, this indicates that there is no homogeneous catalyst in the reaction solution and **1a** is a real heterogeneous catalyst.

In the optimized conditions of the ambient temperature, the catalyst of 0.1 mol%, 2 equivalent TMSCN, and nine carbonyl substrates involving aromatic, aliphatic aldehydes as well as the cycloketones were cyanated. The results obtained are summarized in Table 3, indicating that the reaction is extensively tolerated to various substrates. With standard conditions, the aromatic aldehydes containing distinct substituents or electronic effect substituents (NO_2, OCH_3) were used. After reacting for nine-12 h, the product yield was over

Table 2: Conditions optimization of catalyst **1a** and the comparison test for **1**

Entry	Cat. (mol%)	TMSCN	Temp. (°C)	Conv.[a] (%)
1	0	2 eq.	40	36.6
2	1	2 eq.	40	65.2
3	1	2 eq.	r.t.	76.6
4	0.5	2 eq.	r.t.	96.5
5	0.1	2 eq.	r.t.	98.5
6	0.1 (**1**)	2 eq.	r.t.	38.2

[a] Detected via GC according to carbonyl substrate.

Table 3: The cyanation of TMSCN[a] with different carbonyl compounds

Entry	R_1	R_2	Time (h)	Conv.[b] (%)
1	Ph	H	12	98 (Figure S2)
2	3-$CH_3OC_6H_4$	H	12	90 (Figure S3)
3	4-$CH_3OC_6H_4$	H	12	68 (Figure S4)
4	2-$NO_2C_6H_4$	H	9	100 (Figure S5)
5	2-Furyl	H	20	93 (Figure S6)
6	$(CH_2)_7$	H	40	85 (Figure S7)
7	1-Naphthyl	H	40	64 (Figure S8)
8	9-Anthryl	H	48	19 (Figure S9)

[a]The reaction conditions are **1a** which is 0.003 g and 0.1 mol%, aldehyde/ketone of 0.5 mmol, Me_3SiCN of 1.0 mmol, ambient temperature, under nitrogen atmosphere. [b]Detected via GC and H^1NMR based on carbonyl substrate.

80%, which reveals that the aromatic aldehyde with an electron-deficient group could achieve more effective transformation. Nevertheless, with standard conditions, in comparison with aromatic aldehydes, aliphatic aldehydes have lower catalytic ratio due to their inherent lessened reactivity. After 2 days of reaction, the caprylic aldehyde conversion was only 85% of that of the cyanation. At the aim of investigating and explaining the excellent catalytic activity for open Zn^{2+} positions, **1** was determined under identical reaction conditions; the conversion of the reaction is 38.2%, which is close to the conversion without a catalyst. This is owing to the saturated octahedral configuration of all ions Zn^{2+} in **1**. The obtained results also exhibited that the coordination unsaturated Zn^{2+} positions in **1** possess the important function during catalytic. As the "microreactor," the channel of complex **1** offers a good surrounding for cyanation. As an unsaturated Zn^{2+} position of Lewis acids, it may cause the adsorption preference of the aromatic substrates, therefore improving the catalyst **1a** activity.

3.3 Compound increased the mi-RNA16 relative expression in CP70 ovarian cancer cells

As a regulator of the cancer cell development, the mi-RNA16 could negatively regulate the development of the ovarian cancer cells, which is also used as the biomarker of the ovarian cancer cell detection. Thus, in this research (Figure 3), the mi-RNA16 relative expression level in the cancer cells of CP70 ovarian was measured with RT-PCR. And the results indicated that the compound could significantly increase the expression level of mi-RNA16 in the cancer cells of CP70 ovarian, which is even stronger than the positive anticancer drug Cisplatin, and this anticancer activity showed time-dependent relationship.

3.4 Compound reduced the migration and invasion ability of the CP70 ovarian cancer cells

In the former obtained results, we can find that compound has outstanding induction ability against

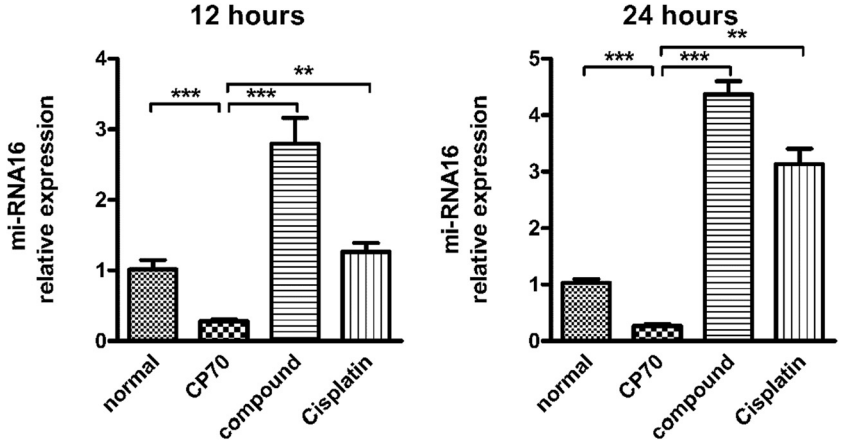

Figure 3: Increased the mi-RNA16 relative expression in the cancer cells of CP70 ovarian after treated by the compound. The CP70 ovarian cancer cells were inoculated into plates of 6 well and carried out compound treatment for half a day and 1 day. The relative expression level of the mi-RNA16 in CP70 ovarian cancer cells was measured with RT-PCR. **means $p < 0.01$, ***means $p < 0.001$.

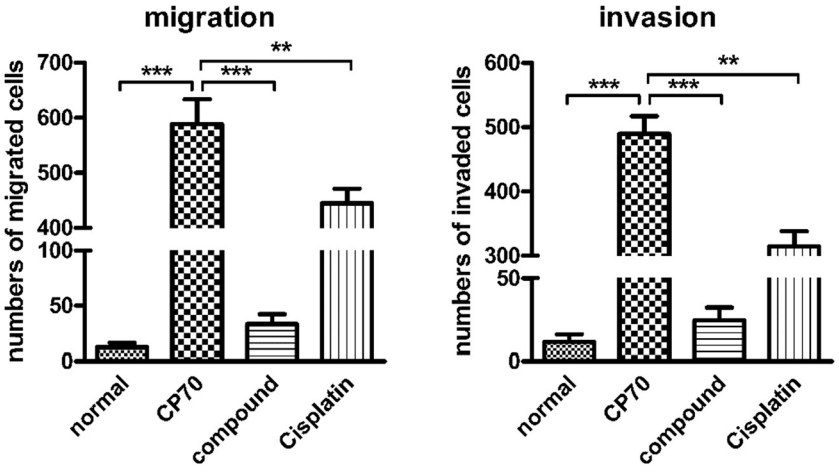

Figure 4: Reduced invasion and migration of the cancer cells of CP70 ovarian after treated with the compound. The CP70 ovarian cancer cells were inoculated into 6 well plates and carried out compound treatment. The migration and invasion of cancer cells of CP70 ovarian were determined with transwell assay. **means $p < 0.01$, ***means $p < 0.001$.

the relative expression of mi-RNA16 in CP70 ovarian cancer, suggesting that compound may possess anticancer activity. The migration and invasion of the cancer cell displayed the malignancy of tumor cells [23]. Thus, in this research, the transwell assay was conducted to detect the compound anti-cancer activity *in vitro*. The data in Figure 4 suggested that the compound obviously reduced the migration and invasion of cancer cells of CP70 ovarian, which is even better than Cisplatin. All the results above demonstrated the compound antitumor ability on cancer cells.

4 Conclusion

In summary, we have produced the metal-organic cage through the reaction between H_3L ligand and Zn $(NO_3)_2{\cdot}6H_2O$ in the mixed solvent of DMF and water. The investigation of the single crystal diffraction of X-ray indicates that complex **1** is composed of eight semi-rigid ligands L and six $Zn_2(CO_2)_4$ structural units to provide the metal-organic cage with the window size of 0.9 nm and the inner diameter of 1.6 nm. The heterogeneous catalytic activities of the complex **1** for aldehydes cyanosilylation in the conditions of solvent-free were studied, which reveals that it could be applied as an effective catalyst for the cyanosilylation reaction under the solvent-free conditions. In biological research, we determined the compound anticancer activity *in vitro*. The real-time RT-PCR results suggested that the compound could significantly increase the expression level of mi-RNA16 in a time-dependent manner, which is important to inhibit the cancer cell progression. In addition to this, the results of the cancer cell migration and invasion ability also suggested that the compound has an inhibitory ability on the cancer cells.

Conflict of interest: Authors declare no conflict of interest.

References

[1] Dong F, Xie X, Wei X, Jiao MM, Duan J, Pan L, et al. Metastatic serous borderline tumor with micro-invasive ovarian carcinoma presenting as a breast lump: a case report. Medicine. 2020;99:e19383.

[2] Honkala AT, Tailor D, Malhotra SV. Guanylate-binding protein 1: an emerging target in inflammation and cancer. Front Immunol. 2020;10:3139.

[3] Noorimotlagh Z, Mirzaee SA, Martinez SS, Rachoń D, Hoseinzadeh M, Jaafarzadeh N. Environmental exposure to nonylphenol and cancer progression risk – a systematic review. Environ Res. 2020;184:109263.

[4] Bacalbasa N, Balescu I, Dimitriu M, Iliescu L, Diaconu C, Dima S, et al. The influence of the preoperative status on the risk of postoperative complications after cytoreductive surgery for advanced-stage ovarian cancer. In Vivo. 2020;34:839–44.

[5] Neogi S, Sharma MK, Bharadwaj PK. Knoevenagel condensation and cyanosilylation reactions catalyzed by a MOF containing coordinatively unsaturated Zn(II) centers. J Mol Catal A Chem. 2009;299:1–4.

[6] Ladrak T, Smulders S, Roubeau O, Teat SJ, Gamez P, Reedijk J. Manganese-based metal-organic frameworks as heterogeneous catalysts for the cyanosilylation of acetaldehyde. Eur J Inorg Chem. 2010;2010:3804–12.

[7] Choi IH, Kim Y, Lee DN, Huh S. Three-dimensional cobalt(II) and cadmium(II) MOFs containing 1,4-naphthalenedicarboxylate: catalytic activity of Cd-MOF. Polyhedron. 2016;105:96–103.
[8] Du JJ, Zhang X, Zhou XP, Li D. Robust heterometallic MOF catalysts for the cyanosilylation of aldehydes. Inorg Chem Front. 2018;5:2772–6.
[9] Feng X, Feng YQ, Liu L, Wang LY, Song HL, Ng SW. A series of Zn-4f heterometallic coordination polymers and a zinc complex containing a flexible mixed donor dicarboxylate ligand. Dalton Trans. 2013;42:7741–54.
[10] Feng X, Ling XL, Liu L, Wang LY, Ng SW, Su BY. A series of 3D lanthanide frameworks constructed from aromatic multicarboxylate ligand: structural diversity, luminescence and magnetic properties. Dalton Trans. 2013;42:10292–303.
[11] Feng X, Xu C, Wang Z, Tang S, Fu W, Ji B, et al. Aerobic oxidation of alcohols and the synthesis of benzoxazoles catalyzed by a cuprocupric coordination polymer (Cu + -CP) assisted by TEMPO. Inorg Chem. 2015;54:2088–90.
[12] Feng X, Ma LF, Liu L, Xie SY, Wang LY. A series of heterometallic three dimensional frameworks constructed from imidazole dicarboxylate: structures, luminescence and magnetic property. Cryst Growth Des. 2013;13:4469–79.
[13] Wang Z, Zhang X, Jiang S, Qu Y, Ou D, Wang J. Arc erosion dynamic of island-and skeleton-restricted microstructure evolution modes in Ag–CuO contact materials. J Alloys Compd. 2020;828:154412.
[14] Duan C, Yu Y, Xiao J, Zhang X, Li L, Yang P, et al. Water-based routes for synthesis of metal–organic frameworks: a review. Sci China Mater. 2020;63:667–85.
[15] Kang YH, Liu XD, Yan N, Jiang Y, Liu XQ, Sun LB, et al. Fabrication of isolated metal–organic polyhedra in confined cavities: adsorbents/catalysts with unusual dispersity and activity. J Am Chem Soc. 2016;138:6099–102.
[16] Huang J, Liu L, Yang Y, Li Y, Wang L, Xiang S, et al. A metal organic cage with semi-rigid ligand for heterogeneous alcoholysis of epoxides. Inorg Chem Commun. 2019;108:107540.
[17] Sheldrick GM. SHELXS-2014, Program for Crystal Structure Solution. Göttingen, Germany: University of Göttingen; 2014.
[18] Sheldrick GM. Crystal structure refinement with SHELXL. Acta Crystallogr C. 2015;71:3–8.
[19] Hu Y, Ding M, Liu XQ, Sun LB, Jiang HL. Rational synthesis of an exceptionally stable Zn(II) metal–organic framework for the highly selective and sensitive detection of picric acid. Chem Commun. 2016;52:5734–7.
[20] Ma Y, Han Z, He Y, Yang L. A 3D chiral Zn(II) coordination polymer with triple Zn–oba–Zn helical chains (oba = 4,4′-oxybis(benzoate)). Chem Commun. 2007;73:4107–9.
[21] He H, Song Y, Sun F, Bian Z, Gao L, Zhu G. A porous metal–organic framework formed by a V-shaped ligand and Zn (II) ion with highly selective sensing for nitroaromatic explosives. J Mater Chem A. 2015;4:1166–9.
[22] Zhang Z, Chen J, Bao Z, Chang G, Xing H, Ren Q. Insight into the catalytic properties and applications of metal–organic frameworks in the cyanosilylation of aldehydes. RSC Adv. 2015;5:79355–60.
[23] van de Merbel AF, van der Horst G, Buijs JT, van der Pluijm G. Protocols for migration and invasion studies in prostate cancer. Methods Mol Biol. 2018;1786:67–79.